Use of metallurgical waste as a catalyst in electro-Fenton process for degradation of dyes from aqueous solution

Hadjer Belbel[a], Rachid Delimi[a], Zahia Benredjem[a,*], Tahar Tayebi[b]

[a]*Laboratory of Water Treatment and Valorization of Industrial Wastes, Department of Chemistry, Faculty of Sciences, Badji Mokhtar-Annaba University, Annaba, Bp 12, 23000, Algeria, emails: z.benredjem@gmail.com (Z. Benredjem), belbel.hadjer@univ-annaba.org (H. Belbel), rachid.delimi@univ-annaba.dz (R. Delimi)*
[b]*Faculty of Sciences and Technology, Mohamed El Bachir El Ibrahimi University, Bordj Bou Arreridj, El-Anasser, 34030, Algeria, email: tahartayebi@gmail.com*

ABSTRACT

As the exploitation of industrial waste has regained interest in recent years for economic and environmental reasons, the valorization of by-products is now part of the sustainable development. This makes it possible to enhance the ethical image of companies and establish commitment towards nature and society. Replacing some chemicals by recovered waste can help in solving the problem partially. Thus, the present work studies the use of metallurgical waste $FeSO_4 \cdot 7H_2O$ as a catalyst in the degradation of the black azo dye eriochrome T (EBT) by the electro-Fenton process. The powder of the $FeSO_4 \cdot 7H_2O$ waste was characterized by X-ray diffraction and scanning electron microscopy. The study of the effect of operating parameters on the efficiency of the EF revealed optimal values for catalyst dose (0.038 g·L^{-1}), supporting electrolyte concentration (8×10^{-3} M) and current density (15 mA·cm^{-2}). The 60 min treatment of 50 mg·L^{-1} EBT solution under optimal operating conditions led to a color and COD removal efficiency of 86.79% and 83.01%, respectively. The results obtained were promising and are of great interest for the use of $FeSO_4 \cdot 7H_2O$ metallurgical waste as a catalyst in the electro-Fenton process.

Keywords: Electro-Fenton; Wastewater treatment; Electrochemical advanced oxidation process; Organic persistent pollutants
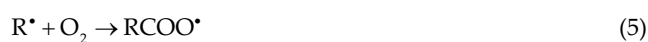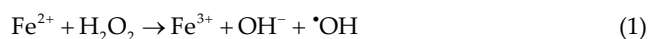
1. Introduction

The increasing use of synthetic dyes in different industries (textile, leather, cosmetics, printing, paper making and paint manufacturing) has made these dyes one of the main sources of water contamination [1]. Among the various dyes, azo dyes account for more than 50% of the world's dye production [2]. Several studies have shown that azo dyes have carcinogenic effects on humans and animals [3,4]. Conventional methods applied for the removal of dyes from wastewater have some disadvantages, for example, adsorption on activated carbon only shifts the pollution from a liquid phase to a solid phase [5], the coagulation/ flocculation process generates huge amounts of sludge at the end of the treatment, which requires additional investments for its treatment [6] it has also been noticed that chemical oxidation is not efficient enough for the treatment of persistent organic pollutants. Therefore, in order to effectively remove the refractory organic pollutant and to consume less chemical reagents, the electro-Fenton (EF) process is used.

Electro-Fenton is based on the production of hydroxyl radicals •OH [7] by the Fenton reaction (1) [8,9], the formation of hydrogen peroxide (2) and the regeneration of ferrous ions at the cathode (3) [8,10]. The effectiveness of the EF process in the treatment of colored solutions has been reported in several works [6,9,11]. The degradation

* Corresponding author.

mechanism of an organic RH compound could be illustrated by equations (4–7) [12]. The rapid attack of hydroxyl radicals on RH molecules occurs essentially by hydrogen atom abstraction from C–H, N–H or OH bonds (4,5), or by addition on a double bond or aromatic rings (ArH) (6,7) [13,14]. In the case of a compound with an azo group, the hydroxyl radical can attack the azo group by hydroxylation [15].

$$Fe^{2+} + H_2O_2 \rightarrow Fe^{3+} + OH^- + {}^{\bullet}OH \tag{1}$$

$$O_2 + 2H^+ + 2e^- \rightarrow H_2O_2 \tag{2}$$

$$Fe^{3+} + e^- \rightarrow Fe^{2+} \tag{3}$$

$$RH + {}^{\bullet}OH \rightarrow R^{\bullet} + H_2O \tag{4}$$

$$R^{\bullet} + O_2 \rightarrow RCOO^{\bullet} \tag{5}$$

$$C=C + {}^{\bullet}OH \rightarrow {}^{\bullet}C\text{-}C\text{-}OH \tag{6}$$

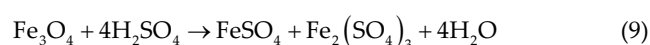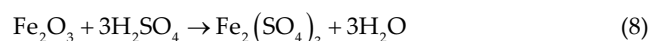$$ArH + {}^{\bullet}OH \rightarrow ArH(OH)^{\bullet} \tag{7}$$

However, during the last three decades, this homogeneous process has undergone modifications. In order to overcome certain limitations, such as the concentration of the catalyst, the restriction of pH 3 and others, many studies have proposed to replace the iron salt with natural minerals: goethite, hematite, magnetite, ferrihydrite, and pyrite. Pyrite, for example, in addition to the possibility of recovering the natural catalyst by filtration, enables in the presence of oxygen, to self-regulate the concentration of iron and to apply the heterogeneous electro-Fenton without adjusting the pH of the solution.

The cost of EF treatment and the policy of environmental friendliness and pollution reduction may be reasons for making changes to the conventional process; for example, replacing the chemical (FeSO4) with an industrial waste. Currently, several countries have imposed new regulations to limit and solve the pollution problem caused by the non-effective use of industrial waste; others adopt the Green Manufacturing philosophy, which is a method of manufacturing that reduces the wastes and pollution in product manufacturing [16]. Indeed, several residues have been used as a renewable source of energy or have been reused as chemical compounds. For example, food industry [17,18], construction renovation and demolition CRD [19], wastewater treatment [20], and steel industries [21,22], agro-industry [23], textiles [24] and others [25,26]. The importance of these products lies in their abundance and low cost.

In the context of industrial waste recovery, we were interested in the iron and steel industry, which, in addition to slag and steel slag, produces other wastes such as iron sulphate during the regeneration of the sulphuric acid pickling bath by cold crystallization. Acid baths are used in metals industries in a process called "stripping". The

various acids such as HNO_3, HF, HCl or H_2SO_4 are used for this purpose as pickling liquor [27,28]. In use, pickling acids gradually enriched with metallic ions become depleted in protons (acid free). In this case, the bath efficiency of stripping decreases [29]. The replacement of the acid used by a new acid generates discharges pollutants and makes the process less economical processing. In the case of using a sulfuric acid pickling bath, regeneration of the bath by cold crystallization produces iron sulphate waste [30]. Stripping with sulfuric acid at 20%–25% and at 95°C–100°C [31] takes place with the dissolution of iron oxide according to the following reactions (8–11) [32].

$$Fe_2O_3 + 3H_2SO_4 \rightarrow Fe_2(SO_4)_3 + 3H_2O \tag{8}$$

$$Fe_3O_4 + 4H_2SO_4 \rightarrow FeSO_4 + Fe_2(SO_4)_3 + 4H_2O \tag{9}$$

$$FeO + H_2SO_4 \rightarrow FeSO_4 + H_2O \tag{10}$$

$$Fe + Fe_2(SO_4)_3 \rightarrow 3FeSO_4 \tag{11}$$

Treatment and recycling of spent bath effluents is possible; for example, Chekioua et al. [30] worked on the regeneration of a synthetic acid bath using electrodialysis process. The objective of this work is to show that a metallurgical waste can be used instead of the FeSO4 catalyst in the EF process. Thus, in this article, we study the possibility of replacing the chemical FeSO4 commonly used as a catalyst in EF by a metallurgical waste for the degradation of a persistent azo dye eriochrome black T (EBT). The metallurgical waste is characterized by SEM-EDS and XRD and the effect of certain operating parameters on the efficiency of the EF process has also been studied.

2. Experimental section

2.1. Chemicals

The dyestuff solution was prepared dissolving 100 mg·L^{-1} of EBT in bi-distilled water, sodium sulfate used as supporting electrolyte Na_2SO_4 was supplied by Sigma-Aldrich, and other reagents used for COD determination including potassium dichromate ($K_2Cr_2O_7$), mercuric sulfate ($HgSO_4$), sulfuric acid (H_2SO_4), silver sulfate (Ag_2SO_4) were purchased from Merck. The carbon felt was purchased from Carbone Lorraine. The ASTM standard stainless steel plates (18% chromium and 10% nickel) were supplied by the company Myriad Distribution (Algeria). All reagents were used without further purification. The metallurgical waste, tested in this work as a catalyst for the Fenton reaction, came from the steel complex, Sider-El-hadjar-Annaba (Algeria) (Fig. 1).

2.2. Experimental and analysis methods

2.2.1. Experimental setup

Electro-Fenton EBT degradation study was carried out in an open reactor consisting essentially of a cylindrical
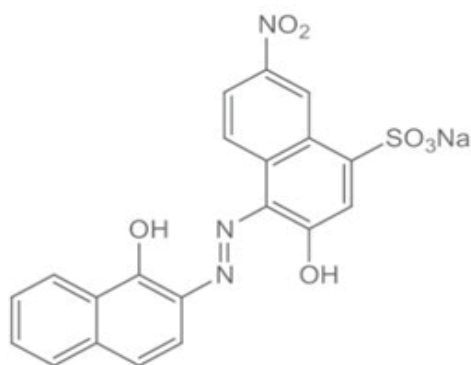
Fig. 1. Eriochrome black T molecule.

cell (200 mL capacity) in which the carbon felt cathode and the stainless steel anode were placed. The two electrodes with effective surfaces 31 cm^2 were spaced 3 cm apart. Electrolysis in galvanostatic mode was performed at ambient temperature using a power supply (VOLTCRAFT PS 405Pro). The current intensity was monitored with an ammeter (metrix MX52). Experiments were conducted in batch mode and the solution was continuously mixed by a magnetic stirrer. Oxygen was supplied to the solution by bubbling (0.2 L·min^{-1}) compressed and purified air during and 10 min before the start of electrolysis. The solution contained a well-defined amount of the catalyst (FeSO$_4$·7H$_2$O) and Na$_2$SO$_4$ as the metallurgical waste supporting electrolyte. The pH was adjusted to 3 using 0.1 M of H$_2$SO$_4$. At given intervals, 5 mL samples were taken from the electrochemical reactor and the EBT concentration, and the COD was analyzed immediately. All the results were expressed as an average of three replicates.

2.2.2. Analysis methods

Color removal was monitored by measuring the reduction in absorbance at wavelength of 540 nm using a spectrophotometer (SPECORD 200). pH was measured using a HANNA instruments 211 pH-meter. The color removal rate of EBT was calculated from Eq. (12). Where A_0 and A_t are the absorbance at initial time and at time t, respectively.

$$\text{Color removal rate}\left(\%\right) = \frac{A_0 - A_t}{A_0} \times 100 \tag{12}$$

The limit of detection (LOD) and limit of quantification (LOQ) of the EBT concentration by the spectrophotometric method using the SPECORD 200 spectrophotometer are 2.04 and 6.82 mg·L^{-1}, respectively.

Solution mineralization efficiency was monitored by measuring its COD evolution. COD was determined using a thermoreactor (WTW CR 2200) and the spectrophotometer. The method is given in previous articles [33,34]. The absorbance value of the excess dichromate is translated into COD. The COD removal rate was calculated according to Eq. (13). Where COD$_0$ and COD$_t$ are respectively, the solution COD values at initial and t time of the electrolysis.

$$\text{COD removal rate}\left(\%\right) = \frac{\text{COD}_0 - \text{COD}_t}{\text{COD}_0} \times 100 \tag{13}$$

In terms of kinetic analysis, the data were analyzed using the pseudo-first-order equation:

$$\ln\left(\frac{C_0}{C_t}\right) = k_1 t \tag{14}$$

And the pseudo-second-order equation:

$$\frac{1}{C_t} = k_2 t + \frac{1}{C_0} \tag{15}$$

C_0, C_t: concentration at time $t = 0$ and time t respectively.
k_1, k_2: constant of pseudo-first equation (min^{-1}) and pseudo-second equation (m^{-1}·min^{-1}) respectively.

3. Results and discussion

3.1. Characterization of the metallurgical waste

3.1.1. SEM and EDS

The thermo scientific quattro environmental scanning electron microscope (ESEM) was used to analyze and confirm the surface morphology of the metallurgical waste. SEM images (Fig. 2) of the metallurgical waste powder show crystals in the form of capillary fiber aggregates with a clear homogeneous surface (Fig. 3).

In addition to the Fe, S and O peaks from the FeSO$_4$, the EDS spectrum contains trace amounts of C and Te. All steels contain C and sometimes additives such as Te. The elements Fe, C and Te were derived from the pickling of the steel with sulphuric acid. The O/Fe atomic number ratio in the presumed FeSO$_4$·7H$_2$O chemical structure is 11:1 while the O/Fe atomic percentage ratio value obtained by EDS is 54.39/3.16 = 17.5 (Table 1). This result suggests that oxygen was also present in other compounds such as carbonates (CO$_3^{2-}$).

3.1.2. X-ray diffraction

To characterize the crystalline structure of the metallurgical waste powder by XRD we used diffractometer PAN analytical diffractometer Empyrean with CuKα = 1.5406 using software programs DataCollector and HighScore Plus both of PANalytical. The values of the peak intensities and their position in the diffractogram of the metallurgical waste sample (Fig. 4) are given in Table 2. The correspondence of the 2θ values of the peaks obtained with those standards of iron sulphate heptahydrated (FeSO$_4$·7H$_2$O) was evaluated with a score of 16.

3.2. Effect of different operating parameters on the EBT degradation using metallurgical waste

In order to optimize the operating conditions for the removal of EBT by electro-Fenton using a metallurgical
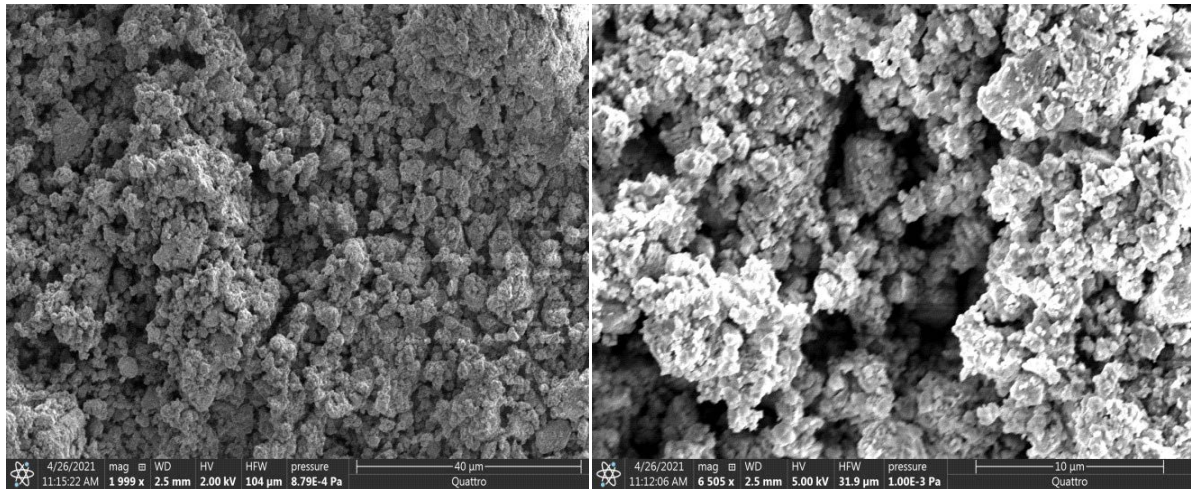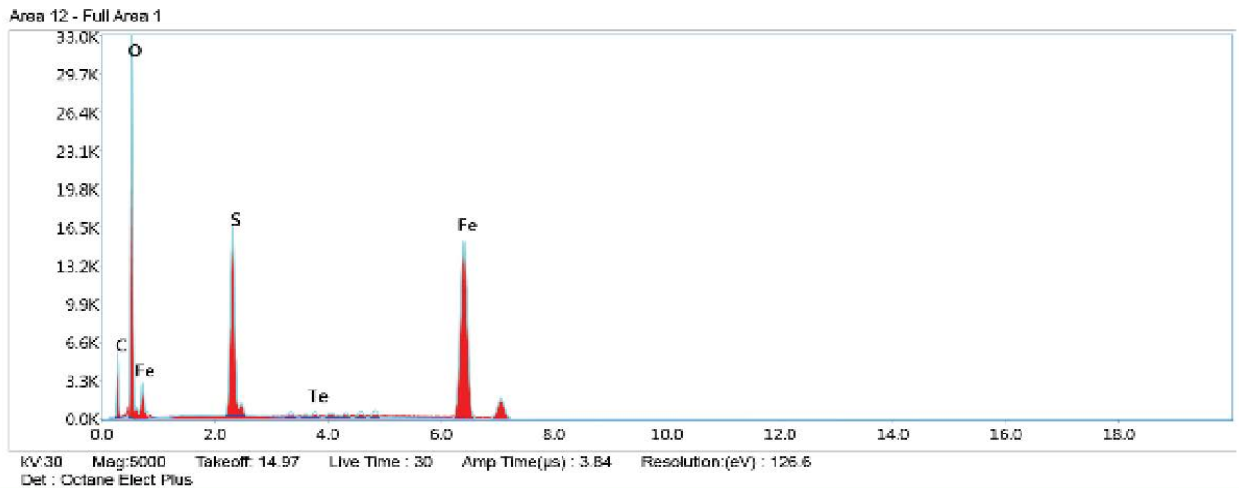
Fig. 2. SEM images of the metallurgical waste.

Fig. 3. Metallurgical waste EDS.

Table 1
Results of metallurgical waste EDS analysis

Element	Weight %	Atomic %	Error %	R
C K	29.32	39.30	10.98	0.9104
O K	54.96	55.29	10.26	0.9197
S K	4.38	2.20	4.72	0.9443
Fe K	10.96	3.16	1.59	0.9646
Te L	0.38	0.05	3.48	0.9554

waste as catalyst, we studied the effect of certain operating parameters on the degradation efficiency of EBT.

3.2.1. Effect of EBT concentration

The effect of the initial dye concentration on the efficiency of EBT degradation by electro-Fenton using $FeSO_4 \cdot 7H_2O$ metallurgical waste as catalyst was investigated for different EBT concentrations in the range 10–100 mg·L^{-1}.

Fig. 5 shows that the decolourization (a) and mineralization (b) efficiencies decrease with increasing EBT concentration. Comparison of the decolourization or mineralization curves at different EBT concentrations shows that the effect of concentration is not very significant. For example, for the concentrations 10 and 100 mg·L^{-1} and after 60 min of treatment, the removal efficiencies for color are 77.93% and 89.36% and for COD are 73.24% and 87.77%, respectively. The decrease in efficiency with increasing EBT concentration was probably largely due to the decrease in the $^{\bullet}OH$/EBT ratio resulting from the increase in EBT concentration. Moreira et al. [8] also observed a low efficiency of the EF process at high pollutant concentrations.

3.2.2. Effect of the metallurgical waste dosage

In order to optimize the concentration of the catalyst waste, making it possible to obtain optimum efficiency of the process and a minimum excess of iron in the treated solution, we carried out experiments on the degradation of EBT by EF for different doses of metallurgical waste ($FeSO_4 \cdot 7H_2O$)
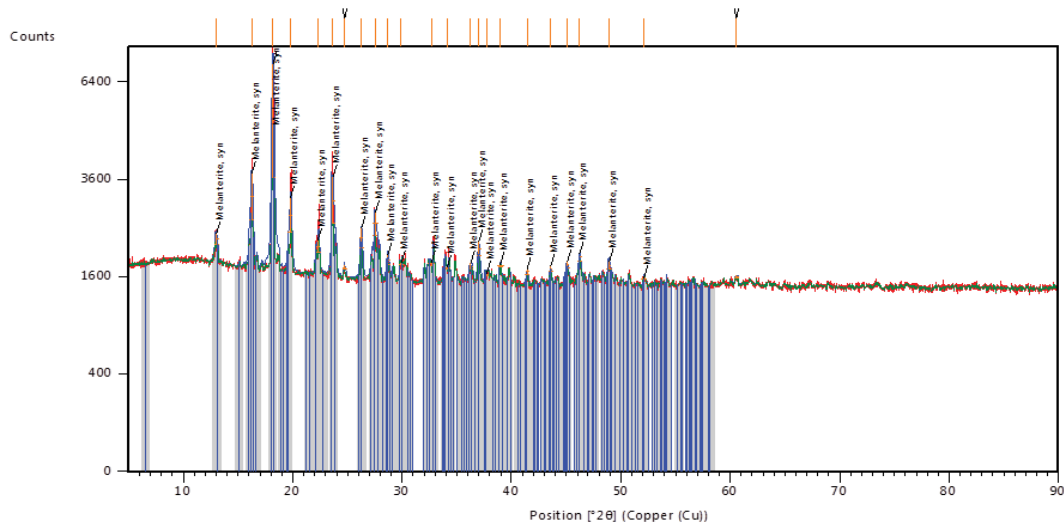
Fig. 4. XRD diffractogram of the metallurgical waste.

Table 2
Values of 2θ, the *d*-spacing and the peaks size of the metallurgical waste powder

	Pos. (°2θ)	Height (cts)	FWHM left (°2θ)	*d*-spacing (Å)		Rel. Int. (%)
	12.9967	208.00	0.3070	6.81191		6.20
	16.2313	1,068.46	0.3070	5.46100		31.83
	18.1931	3,357.27	0.3070	4.87629		100.00
	19.7907	749.21	0.3070	4.48612		22.32
	22.2950	225.93	0.3070	3.98757		6.73
	23.6824	1,064.85	0.3070	3.75700		31.72
	24.7345	78.31	0.3070	3.59953		2.33
	26.2613	391.26	0.3070	3.39362		11.65
	27.5429	482.03	0.5117	3.23856		14.36
	28.6947	177.17	0.3070	3.11113		5.28
	29.8880	27.61	0.3070	2.98958		0.82
	32.6611	52.82	0.6140	2.74181		1.57
	34.0958	20.76	0.5117	2.62965		0.62
	36.2656	97.87	0.3582	2.47714		2.92
	37.0040	272.79	0.3070	2.42939		8.13
	37.7484	32.12	0.3070	2.38318		0.96
	38.9499	34.63	0.6140	2.31238		1.03
	41.4170	87.97	0.3070	2.18017		2.62
	43.5372	87.67	0.3070	2.07879		2.61
	45.0814	98.31	0.2558	2.01111		2.93
	46.2200	149.34	0.3070	1.96418		4.45
	48.9329	137.51	0.3070	1.86145		4.10
	52.1249	18.46	0.3070	1.75472		0.55
	60.5670	60.34	0.3070	1.52879		1.80
Visible	Ref. Code	Score name	Compound	Displ. (°2θ)	Scale Fac.	Chem. formula
*	01-076-0657	16	Iron sulfate hydrate	0.000	0.325	$Fe(SO_4)_7(H_2O)$

in range 0.015–0.15 g·L^{-1}. As can be seen in Fig. 6, the catalyst waste dose has a significant effect on the degradation efficiency of EBT. It can be seen that the color and COD removal efficiencies increase from 78.17% and 77.13% to 86.33%

and 80.72% when the catalyst waste dose was increased from 0.015–0.038 g·L^{-1}, and then increasing the dose above 0.038 g·L^{-1} leads to a decrease inefficiencies. It is considered that 0.038 g·L^{-1} is an optimum dose of catalyst waste.
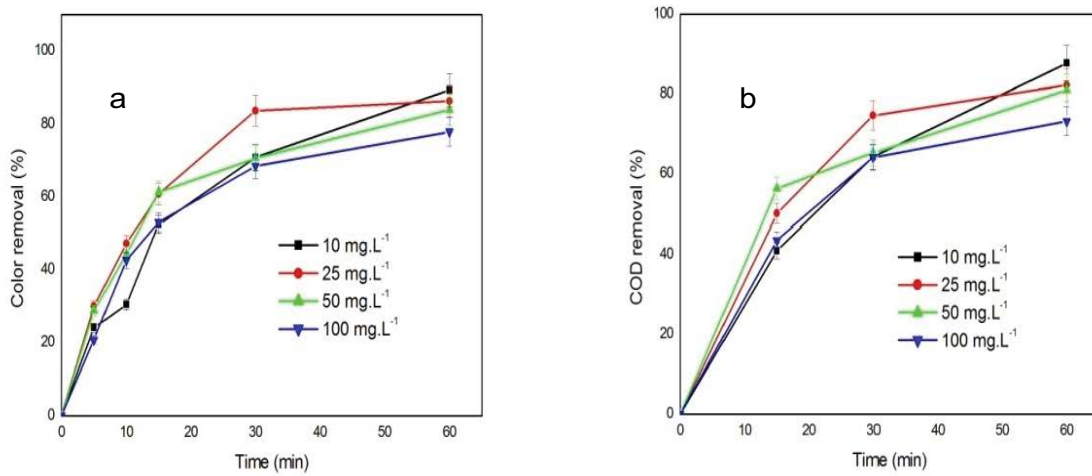
Fig. 5. Effect of EBT concentration on color (a) and COD (b) removal of EBT solution. [$FeSO_4$] waste = 0.038 g·L^{-1}; pH = 3; [Na_2SO_4] = 8 × 10^{-3} M; I = 15 mA·cm^{-2}; V = 200 mL.
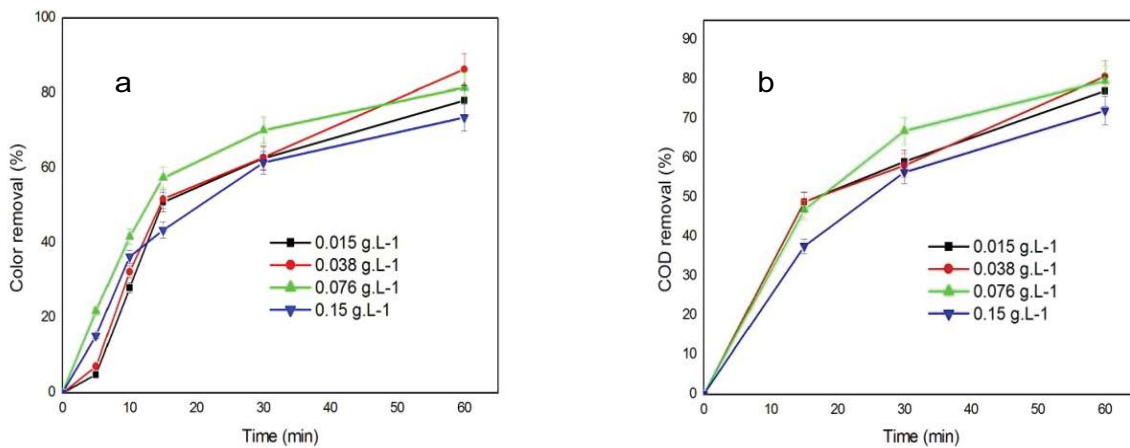

Fig. 6. Effect of waste catalyst dose on color (a) and COD (b) removal of EBT solution. [EBT] = 50 mg·L^{-1}; [Na_2SO_4] = 8 × 10^{-3} M; pH = 3, I = 15 mA·cm^{-2}; V = 200 mL.

The negative effect of strong concentrations of the waste catalyst on the degradation kinetics can be explained by the enhanced reaction that occurs between hydroxyl radicals and excess ferrous ions (16) [7,35]. In addition, the excess of formed Fe^{3+} ions consumes hydrogen peroxide according to reactions (17) and (18) [36,37].

$$Fe^{2+} + {}^\bullet OH \rightarrow Fe^{3+} + OH^- \tag{16}$$

$$Fe^{3+} + H_2O_2 \rightarrow Fe\text{-}OOH^{2+} + H^+ \tag{17}$$

$$Fe\text{-}OOH^{2+} \rightarrow HO_2^\bullet + Fe^{2+} \tag{18}$$

The rate constants k_1 and k_2 and the correlation coefficient R^2 calculated for the pseudo-second-order kinetic models are shown in Table 3. The R^2 values (Table 3) clearly indicate that the pseudo-second-order model gives a better prediction than the pseudo-first-order model for EBT removal.

Table 3
Kinetic analysis of experimental results

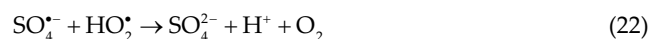| Dose of catalyst waste (g·L^{-1})	Pseudo-first-order		Pseudo-second-order	
	k_1 (min^{-1})	R^2	k_2 (m^{-1}·min^{-1})	R^2
0.015	0.0258	0.9306	0.1144	0.9891
0.038	0.0330	0.9781	0.1921	0.9496
0.076	0.0270	0.9139	0.1345	0.9945
0.150	0.0215	0.9300	0.0855	0.9922

3.2.3. Effect of supporting electrolyte concentration

Sodium sulfate (Na_2SO_4) is the supporting electrolyte commonly used by researchers in EF. However, there is not unanimity on its concentration, which is why we have studied the effect of the Na_2SO_4 concentration on the efficiency of color and COD removal.

Fig. 7 shows the results of the variation of (a) decolourization and (b) mineralization efficiency of the solution with

the concentration of the supporting electrolyte in the range. It can be seen that increasing the concentration of Na_2SO_4 from 4×10^{-3} to 8×10^{-3} M leads to an increase in the color and COD removal rates from 75.83% and 74.51% to 86.79% and 83.01% respectively. This might be explained by the fact that oxidation of SO_4^{2-} at the anode leads to the formation of peroxodisulfate ions (19) that subsequently oxidize EBT molecules which improves their removal [34]. However increasing the concentration from 8×10^{-3}–3.5×10^{-2} M leads to a regression of the color and COD removal up to 76.67% and 75.73% respectively.

We attribute the decrease in color and COD removal efficiencies with increasing supporting electrolyte concentration in the range 8×10^{-3}–3.5×10^{-2} M to the scavenging of hydroxyl radicals and hydrogen peroxide by SO_4^{2-} ions according to reaction (20)–(22) [38].

$$2SO_4^{2-} \rightarrow S_2O_8^{2-} + 2e^- \tag{19}$$

$$^\bullet OH + SO_4^{2-} \rightarrow OH^- + SO_4^{\bullet-} \tag{20}$$

$$SO_4^{\bullet-} + H_2O_2 \rightarrow SO_4^{2-} + H^+ + HO_2^\bullet \tag{21}$$

$$SO_4^{\bullet-} + HO_2^\bullet \rightarrow SO_4^{2-} + H^+ + O_2 \tag{22}$$

The removal efficiency of EBT by electro-Fenton using a metallurgical waste as catalyst is compared with other methods (Table 4). A comparison of the different techniques in terms of efficiency, dye concentration and treatment time shows that, with the exception of biosorption on *Agaricus campestris* (99%), EBT removal by electro-Fenton was the most efficient (87%) and fastest (60 min).

3.2.4. Effect of current density

In electro-Fenton the current density is an important parameter on which the efficiency and cost of the treatment depends. In order to investigate the effect of this parameter on the EBT solution degradation, several current values in the range 5–35 $mA \cdot cm^{-2}$ were applied under the same operating conditions. Fig. 8 shows that after 60 min of treatment by EF of a 50 $mg \cdot L^{-1}$ EBT solution, the variation of the current density from 5 to 15 $mA \cdot cm^{-2}$ leads to an increase in the degradation rate from 70% to 82.25% (Fig. 8a) and an increase in the percentage of COD removal from 68.25% to 80.51% (Fig. 8b). However, increasing the current density from 15 to 35 $mA \cdot cm^{-2}$
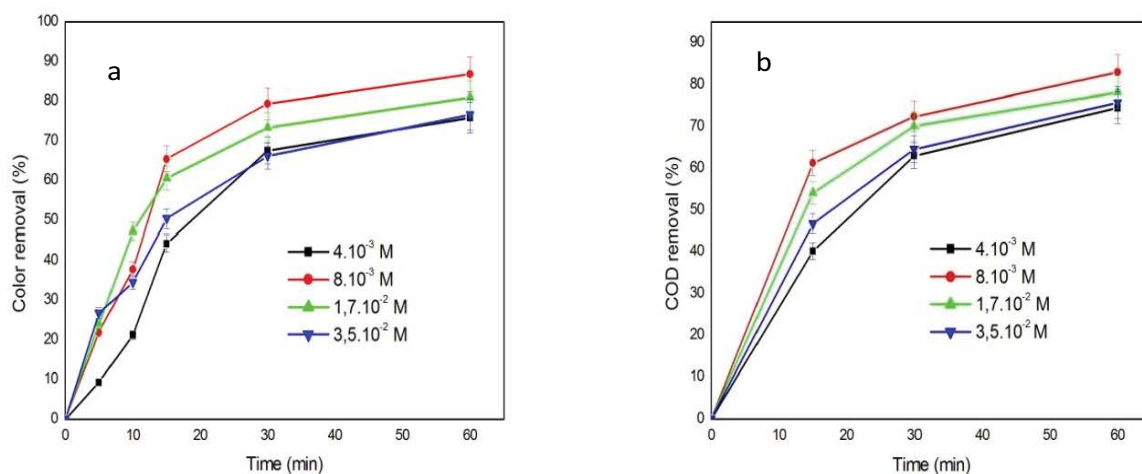

Fig. 7. Effect of supporting electrolyte concentration on color (a) and COD (b) removal. $[FeSO_4]$ waste = 0.038 $g \cdot L^{-1}$; [EBT] = 50 $mg \cdot L^{-1}$; pH = 3; I = 15 $mA \cdot cm^{-2}$; V = 200 mL.

Table 4
Comparison of EBT removal efficiency by electro-Fenton using a metallurgical waste as catalyst with those obtained by other methods

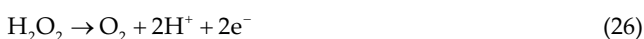| Removal of EBT by	EBT concentration ($mg \cdot L^{-1}$)	Efficiency removal (%)	Time contact (min)	Reference
Adsorption on to eucalyptus bark	100	68	180	Dave et al. [39]
Biosorption on to *Agaricus campestris*	100	99	20	Alp et al. [40]
Adsorption on MnO_2-coated zeolite	20	79	660	Aguila and Ligaray [41]
Photocatalysis on tridoped titanium oxide	20	89	240	Mamba et al. [42]
Adsorption on AlTiPbO nanoparticles	100	86	90	Jethave et al. [43]
Electro-Fenton using metallurgical waste	100	87	60	This study
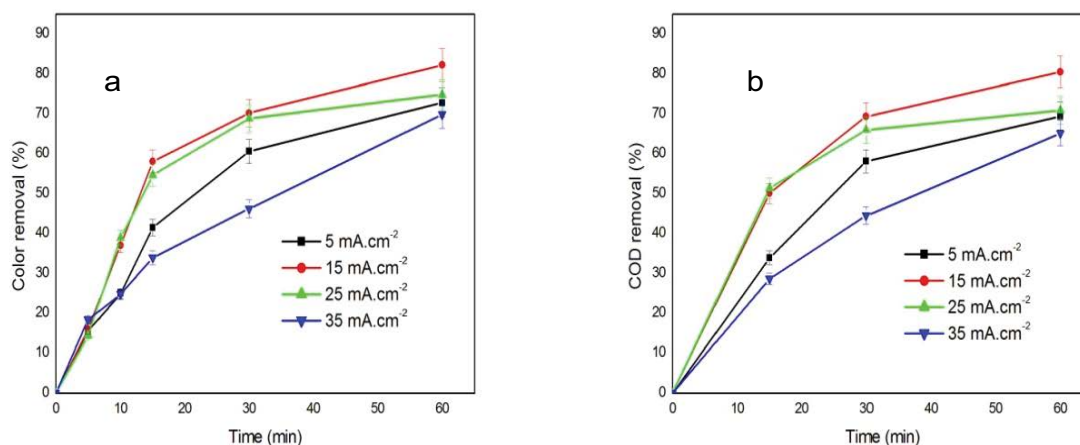
Fig. 8. Effect of current density on color (a) and COD removal (b) of EBT solution. [EBT] = 50 mg·L^{-1}; [FeSO$_4$] waste = 0.038 g·L^{-1}; pH = 3; [Na$_2$SO$_4$] = 8 × 10^{-3} M; V = 200 mL.

leads to a decrease in degradation and mineralization efficiency to 69.90% and 65.20%, respectively. The change in efficiency observed with current density can be interpreted by the fact that increasing the current density up to a certain value, in our case 15 mA·cm^{-2}, increases the efficiency of the process, by accelerating the reduction of oxygen to hydrogen peroxide (2) and the reduction of Fe^{3+} at the cathode to form Fe^{2+}(3) whose concentration controls the production of •OH (1). However, at current density values greater than 15 mA·cm^{-2}, we observed a decrease in the degradation rate due to the intensification of parasitic reactions which competes with the previous reactions: release of hydrogen at the cathode (23); the oxidation of Fe^{2+} at the Fe^{3+} anode (24) and oxidative/reductive decay of H$_2$O$_2$ at the cathode (25) and at the anode (26) [8,44,45].

$$2H^+ + 2e^- \rightarrow H_2(g) \tag{23}$$

$$Fe^{2+} \rightarrow Fe^{3+} + e^- \tag{24}$$

$$H_2O_2 + 2H^+ + 2e^- \rightarrow 2H_2O \tag{25}$$

$$H_2O_2 \rightarrow O_2 + 2H^+ + 2e^- \tag{26}$$

4. Conclusion

Until now, advanced oxidation processes (AOPs) such as EF have not been applied on an industrial scale due to their extremely high cost. In this work, it was shown that the chemical reagent FeSO$_4$ used as a catalyst can be replaced by a metallurgical waste, thus reducing the cost of the EF process. SEM and XRD analysis of the metallurgical waste powder revealed crystals in the form of capillary aggregates with a homogeneous surface and seven times hydrated iron sulphate (FeSO$_4$·7H$_2$O).

The study of the effect of operating parameters on the efficiency of the EF revealed optimal values for catalyst dose (0.038 g·L^{-1}), supporting electrolyte concentration

(8 × 10^{-3} M) and current density (15 mA·cm^{-2}). Using metallurgical waste as a catalyst, color and COD removal efficiencies of 86.79% and 83.01% respectively were achieved after 60 min of EF treatment with a 50 mg·L^{-1} EBT solution.

Finally, this study demonstrated that FeSO$_4$·7H$_2$O metallurgical waste can replace the conventional catalyst in the EF process and reduce its process cost.

References

[1] W.S. Wan Ngah, L.C. Teong, M.A.K.M. Hanafiah, Adsorption of dyes and heavy metal ions by chitosan composites: a review, Carbohydr. Polym., 83 (2011) 1446–1456.

[2] A. Pandey, P. Singh, L. Iyengar, Bacterial decolorization and degradation of azo dyes, Int. Biodeterior. Biodegrad., 59 (2007) 73–84.

[3] B.-Y. Chen, Toxicity assessment of aromatic amines to *Pseudomonas luteola*: chemostat pulse technique and dose–response analysis, Process Biochem., 41 (2006) 1529–1538.

[4] S. Tsuda, N. Matsusaka, H. Madarame, S. Ueno, N. Susa, K. Ishida, N. Kawamura, K. Sekihashi, Y.F. Sasaki, The comet assay in eight mouse organs: results with 24 azo compounds, Mutat. Res., 465 (2000) 11–26.

[5] G. Mckay, G. Ramprasad, P. Mowli, Desorption and regeneration of dye colours from low-cost materials, Water Res., 21 (1987) 375–377.

[6] K. Hasani, M. Moradi, S.A. Mokhtari, H. Sadeghi, A. Dargahi, M. Vosoughi, Degradation of basic violet 16 dye by electroactivated persulfate process from aqueous solutions and toxicity assessment using microorganisms: determination of by-products, reaction kinetic and optimization using Box–Behnken design, Int. J. Chem. Reactor Eng., 19 (2021) 261–275.

[7] M. Panizza, M.A. Oturan, Degradation of Alizarin Red by electro-Fenton process using a graphite-felt cathode, Electrochim. Acta, 56 (2011) 7084–7087.

[8] F.C. Moreira, R.A.R. Boaventura, E. Brillas, V.J.P. Vilar, Electrochemical advanced oxidation processes: a review on their application to synthetic and real wastewaters, Appl. Catal., B, 202 (2017) 217–261.

[9] Z. Benredjem, K. Barbari, I. Chaabna, S. Saaidia, A. Djemel, R. Delimi, S. Douas, K. Bakhouche, Comparative investigation on the removal of methyl orange from aqueous solution using three different advanced oxidation processes, Int. J. Chem. Reactor Eng., 19 (2021) 597, doi: 10.1515/ijcre-2020-0243.

[10] E. Brillas, I. Sires, M. Oturan, Electro-Fenton process and related electrochemical technologies based on Fenton's reaction chemistry, Chem. Rev., 109 (2009) 6570–6631.

[11] P. Nidheesh, M. Zhou, M.A. Oturan, An overview on the removal of synthetic dyes from water by electrochemical advanced oxidation processes, Chemosphere, 197 (2018) 210–227.

[12] H. He, Z. Zhou, Electro-Fenton process for water and wastewater treatment, Crit. Rev. Env. Sci. Technol., 47 (2017) 2100–2131.

[13] J. Pignatello, E. Oliveros, A. Mackay, Advanced oxidation processes for organic contaminant destruction based on the Fenton reaction and related chemistry, Crit. Rev. Env. Sci. Technol., 36 (2006) 1–84.

[14] I. Sires, E. Brillas, M.A. Oturan, M.A. Rodrigo, M. Panizza, Electrochemical advanced oxidation processes: today and tomorrow. A review, Environ. Sci. Pollut. Res., 21 (2014) 8336–8367.

[15] B. Kayan, B. Gözmen, M. Demirel, A.M. Gizir, Degradation of acid red 97 dye in aqueous medium using wet oxidation and electro-Fenton techniques, J. Hazard. Mater., 177 (2010) 95–102.

[16] B. Logesh, M. Balaji, Experimental investigations to deploy green manufacturing through reduction of waste using lean tools in electrical components manufacturing company, Int. J. Green Technol., 8 (2021) 365–374.

[17] B. Bayram, G. Ozcan, T. Kostka, E. Capanogh, T. Esatbeyoglu, Valorization and application of fruit and vegetable wastes and by-products for food packaging materials, Molecules, 26 (2021) 4031, doi: 10.3390/molecules26134031.

[18] V.O. Okoro, L. Nie, P. Hobbi, A. Shavandi, Valorization of waste apple pomace for production of platform biochemicals: a multi-objective optimization study, Waste Biomass Valorization, 12 (2021) 6887–6901.

[19] M.A. Laadila, Y. Le Bihan, R.F. Caron, C. Vaneeckhaute, Construction, renovation and demolition (CRD) wastes contaminated by gypsum residues: characterization, treatment and valorization, J. Waste Manage., 120 (2021) 125–135.

[20] M. Jeguirim, S. Jellali, Wastewater treatment, valorization, and reuse, Water J., 13 (2021) 548, doi: 10.3390/w13040548.

[21] J. Rieger, V. Colla, I. Matino, A.T. Branca, G. Stubbe, A. Panizza, C. Brondi, M. Falsafi, J. Hage, X. Wang, B. Voraberger, T. Fenzl, V. Masaguer, E.L. Faraci, L. di Sante, F. Cirilli, F. Loose, C. Thaler, A. Soto, P. Frittella, G. Foglio, C. di Cecca, M. Tellaroli, M. Corbella, M. Guzzon, E. Malfa, A. Morillon, D. Algermissen, K. Peters, D. Snaet, Residue valorization in the iron and steel industries: sustainable solutions for a cleaner and more competitive future Europe, Metals, 11 (2021) 1202, doi: 10.3390/met11081202.

[22] L.A.H. Alkindi, W.K. Kh. Alghabban, Framework for solid waste management in steel fabrication, J. Eng. Technol., 37 (2019) 227–236.

[23] E. Virmond, J.D. Rocha, R.F.P.M. Moreira, H.J. José, Valorization of agroindustrial solid residues and residues from biofuel production chains by thermochemical conversion: a review, citing Brazil as a case study, Braz. J. Chem. Eng., 30 (2013) 197, doi: 10.1590/S0104-66322013000200001.

[24] G. Xia, W. Han, Z. Xu, J. Zhang, F. Kong, J. Zhang, X. Zhang, F. Jia, Complete recycling and valorization of waste textiles for value-added transparent films via an ionic liquid, J. Environ. Chem. Eng., 9 (2021) 106182, doi: 10.1016/j.jece.2021.106182.

[25] E. Dieckmann, R. Onsiong, B. Nagy, L. Sheldrick, C. Cheeseman, Valorization of waste feathers in the production of new thermal insulation materials, Waste Biomass Valorization, 12 (2021) 1119–1131.

[26] B.E. Sydney, J.C. de Carvalho, L.A.J. Letti, A.I. Magalhães, S.G. Karp, W.J. Martinez-Burgos, E.D.S. Candeo, C. Rodrigues, L.P.D.S. Vandenberghe, C.J.D. Neto, L.A.Z. Torres, A.B.P. Medeiros, A.L. Woiciechowski, C.R. Soccol, Agro-industrial wastewater in a circular economy: characteristics, impacts and applications for bioenergy and biochemicals, J. Hazard. Mater., 341 (2020) 125795, doi: 10.1016/j.biortech.2021.125795.

[27] J. Jinki, K. Min-Seuk, K. Byung-Su, K. Soo-Kyung, K. Won-Baek, C. Jae, Recovery of H_2SO_4 from waste acid solution by a diffusion dialysis method, J. Hazard. Mater., 124 (2005) 230–235.

[28] Z. Palarty, A. Zakova, Separation of $H_2SO_4 + CuSO_4$ mixture by diffusion dialysis, J. Hazard. Mater., 114 (2004) 69–74.

[29] R. Magdalena, W. Maciej, Selective removal of zinc(II) from spent pickling solutions in the presence of iron ions with phosphonium ionic liquid Cyphos IL 101, Hydrometallurgy, 110 (2011) 85–90.

[30] A. Chekiouaa, R. Delimi, Purification of H_2SO_4 of pickling bath contaminated by Fe(II) ions using electrodialysis process, Energy Procedia, 74 (2015) 1418–1433.

[31] K. Yasouhiro, N. Toshiyuki, M. Kazunari, A new synthesis route from spent sulfuric acid pickling solution to ferrite nanoparticles, Hydrometallurgy, 74 (2004) 57–65.

[32] A. Archana, K.K. Sahu, An overview of the recovery of acid from spent acidic solutions from steel and electroplating industries, J. Hazard. Mater., 171 (2009) 61–75.

[33] K. Barbari, R. Delimi, Z. Benredjem, S. Saaidia, A. Djemel, T. Chouchane, N. Oturan, M.A. Oturan, Photocatalytically-assisted electrooxidation of herbicide fenuron using a new bifunctional electrode $PbO_2/SnO_2-Sb_2O_3/Ti//Ti/TiO_2$, Chemosphere, 203 (2018) 1–10.

[34] S. Saaidia, R. Delimi, Z. Benredjem, A. Mehellou, A. Djemel, K. Barbari, Use of a PbO_2 electrode of a lead-acid battery for the electrochemical degradation of methylene blue, Sep. Sci. Technol., 52 (2017) 1602–1614.

[35] M.F. Murrieta, E. Brillas, J.L. Nava, I. Sirés, Photo-assisted electrochemical production of HClO and Fe^{2+} as Fenton-like reagents in chloride media for sulfamethoxazole degradation, Sep. Purif. Technol., 250 (2020) 117236, doi: 10.1016/j.seppur.2020.117236.

[36] O. Ganzenko, N. Oturan, D. Huguenot, E.D. van Hullebusch, G. Esposito, M.A. Oturan, Removal of psychoactive pharmaceutical caffeine from water by electro-Fenton process using BDD anode: effects of operating parameters on removal efficiency, Sep. Purif. Technol., 156 (2015) 987–995.

[37] A. Özcan, Y. Şahin, A. Savaş Koparal, M.A. Oturan, Carbon sponge as a new cathode material for the electro-Fenton process: comparison with carbon felt cathode and application to degradation of synthetic dye basic blue 3 in aqueous medium, J. Electroanal. Chem., 616 (2008) 71–78.

[38] J. De Laat, G. Truong Le, B. Legube, A comparative study of the effects of chloride, sulfate and nitrate ions on the rates of decomposition of H_2O_2 and organic compounds by Fe(II)/H_2O_2 and Fe(III)/H_2O_2, Chemosphere., 55 (2004) 715–723.

[39] P.N. Dave, S. Kaur, E. Khosla, Removal of Eriochrome black-T by adsorption on to eucalyptus barks using green technology, Indian J. Chem. Technol., 18 (2011) 53–60.

[40] H. Alp, M. Ince, O.K. Ince, A. Onal, Biosorptive removal of Eriochrome Black-T using *Agaricus campastris*: parameters optimization with response surface methodology, Desal. Water Treat., 175 (2020) 244–254.

[41] D.M.M. Aguila, M.V. Ligaray, Adsorption of Eriochrome Black T on MnO_2-coated zeolite, Int. J. Environ. Sci. Dev., 6 (2015) 824–827.

[42] G. Mamba, X.Y. Mbianda, A.K. Mishra, Enhanced visible light photocatalytic degradation of Eriochrome Black T and eosin blue shade in water using tridoped titania decorated on SWCNTs and MWCNTs: effect of the type of carbon nanotube incorporated, Mater. Chem. Phys., 149 (2015) 734–742.

[43] G. Jethave, U. Fegade, S. Attarde, S. Ingle, Decontamination study of Eriochrome Black-T from waste water by using AlTiPbO Nanoparticles (ATPO-NPs) for sustainable clean environment, J. Water Environ. Nanotechnol., 4 (2019) 263–274.

[44] N. Oturan, M.A. Oturan, Electro-Fenton Process: Background, New Developments, and Applications, Electrochemical Water and Wastewater Treatment, 2018, pp. 193–221.

[45] H. Zazou, N. Oturan, H. Zhang, M. Hamdani, M.A. Oturan, Comparative study of electrochemical oxidation of herbicide 2,4,5-T: kinetics, parametric optimization and mineralization pathway, Sustainable Environ. Res., 27 (2017) 15–23.